RBN-2397, a novel, potent, and selective PARP7 inhibitor, induces tumor-intrinsic Type I interferon responses and adaptive immunity in patient tumors

[1,8]Kristy G. Kuplast-Barr, [2]Melissa Johnson, [3]Manish R. Patel, [4]Timothy A. Yap, [5]Gerald S. Falchook, [6]Patricia LoRusso, [1]Ryan Abo, [1]Chang Liu, [1]Erika L. Manyak, [1]Lisa Cleary, [1]Viviana Bozon, [1]Sudha Parasuraman, [1]Heike Keilhack, [1,7]Kristen McEachern

[1]Ribon Therapeutics, Cambridge, MA, USA; [2]Sarah Cannon Research Institute, Nashville, TN, USA; [3]Sarah Cannon Research Institute/Florida Cancer Specialists, Sarasota, FL, USA; [4]MD Anderson Cancer Center, Houston, TX, US; [5]Sarah Cannon Research Institute at HealthONE, Denver, CO, US; [6]Department of Medical Oncology, Yale University School of Medicine, Yale Cancer Center, New Haven, CT, USA; [7]Corresponding author; [8]Presenting author

Abstract 1836
AACR 2022

Background

PARP7 is a mono-ART that is upregulated in response to cellular stress (e.g., viral infection, cigarette smoke), and suppresses the Type I interferon (IFN) response following cytosolic nucleic acid sensing. RBN-2397 is a first-in-class PARP7 inhibitor, inducing cancer cell autonomous and immune stimulatory effects in preclinical models through enhanced Type I IFN signaling in cancer cells. Moreover, RBN-2397 induces CD8$^+$ T cell-dependent tumor-specific immune memory in an immunocompetent mouse cancer model[1]. RBN-2397 is currently being tested in an ongoing Phase I clinical study (NCT04053673)[2]. Here we present evidence of proof of mechanism in the paired tumor biopsies from patients in the Phase 1 study.

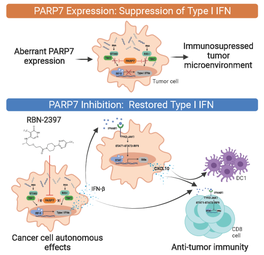

Patient Samples Confirm RBN-2397 Modulates Type I Interferon Signaling in Tumor, not Periphery

RBN-2397-19-001: Phase 1 Dose Escalation with Expansion Cohorts

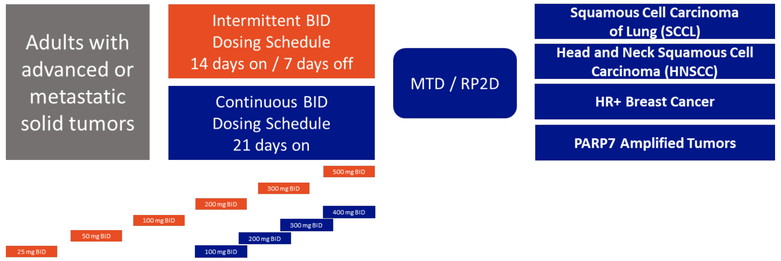

Figure 1. Phase 1 study design. The dose escalation is complete, MTD/RP2D have been established, and enrollment in expansion cohorts is ongoing[2].

RBN-2397 induces expression of ISGs, including CXCL10, in select tumor types based on preclinical data[1,3]

Increases in ISG expression are more prominent in tumor types with higher expression of PARP7

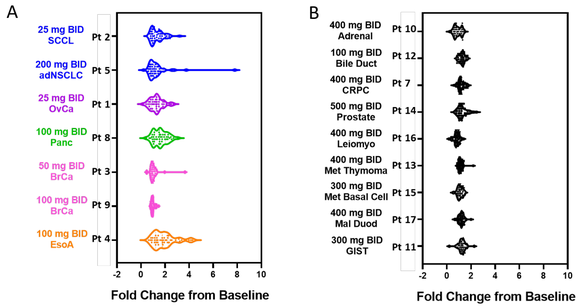

CXCL10 is increased in on-treatment biopsies, but not PBMCs, from patients treated with RBN-2397

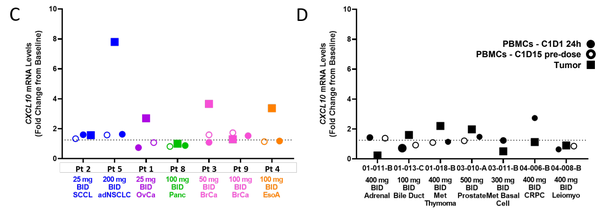

Figure 2. In panels A and B, expression of 42 ISGs was measured by NanoString analysis of on-treatment core needle biopsies from 16 patients with evaluable data treated with RBN-2397 in the dose escalation portion of the on-going Phase 1 study. Panel A highlights tumors of interest such as breast, ovarian, esophageal, lung, and pancreatic, while panel B includes remaining tumor types. In panels C and D, *CXCL10* mRNA expression was measured in peripheral blood cells of the same patients treated with RBN-2397 using NanoString analysis at two timepoints during Cycle 1 or in on-treatment core needle biopsies. Similarly, panel C highlights tumors of interest while panel D includes remaining tumor types. Closed circles represent samples taken 24 hours post-dose on day 1, open circles represent samples taken pre-dose on cycle 1 day 15, and squares represent on-treatment biopsies taken between C1D14 and C2D14. Dotted line signifies 1.25-fold change from baseline.

References
1. Gozgit et al. PARP7 negatively regulates the Type I interferon response in cancer cells and its inhibition triggers antitumor immunity. Cancer Cell. 2021; 39(9):1214-1226
2. Falchook et al. A First-In-Human Phase 1 Study of a Novel PARP7 Inhibitor RBN-2397 in Patients with Advanced Solid Tumors. ASCO 2021 oral presentation
3. Wang et al. Elevated PARP7 expression in select cancers identifies a target population for RBN-2397 therapy. AACR 2021, abstract 381

CD8$^+$ T Cells and Granzyme B expression are increased in on-treatment biopsies of patients treated with RBN-2397, particularly in tumor types with higher expression of PARP7

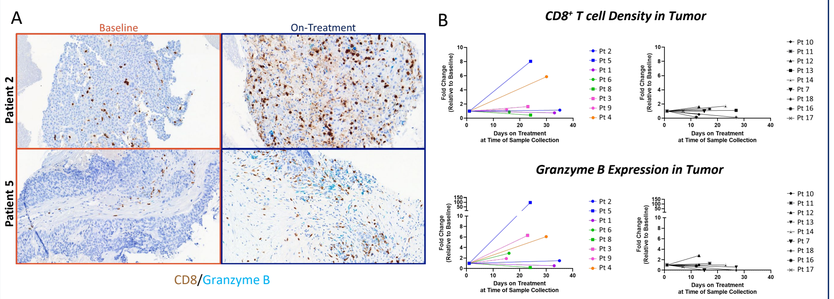

Figure 4. Panel A shows representative 10x images from immunohistochemical staining of CD8 (brown) and Granzyme B (teal) expression in the paired biopsies of two patients with lung cancer taken at baseline and on-treatment during Cycle 2. Patient 1 on-treatment biopsy was taken at Cycle 2 Day 14 from a lung nodule. Patient 2 on-treatment biopsy was taken at Cycle 2 Day 3 from a liver metastasis. In panel B, CD8 and Granzyme B expression were assessed by immunohistochemistry in paired biopsies from 17 patients in the Phase 1 dose escalation study with RBN-2397. Colored graphs highlight tumors of interest such as breast, ovarian, esophageal, lung, and pancreatic, while black and white graphs depict the remainder of the data. Positivity for each marker was quantified by image analysis (HALO) and fold change over baseline was plotted for the on-treatment samples.

CXCL10 is not consistently increased in plasma or PBMCs from patients treated with RBN-2397

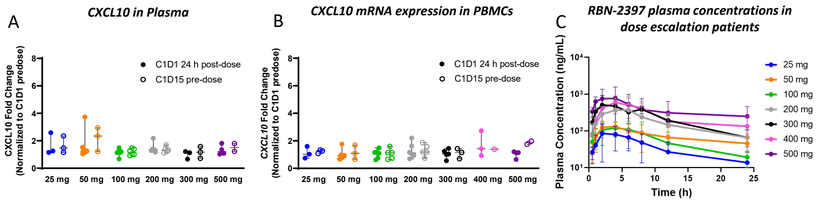

Figure 3. In panel A, CXCL10 was measured in plasma from patients treated with RBN-2397 by MSD analysis at two timepoints during dosing Cycle 1. In panel B, *CXCL10* mRNA expression was measured using NanoString analysis of peripheral blood cells at two timepoints during dosing in Cycle 1. For both assays closed circles represent samples taken 24 hours post-dose on day 1 (n=27/n=32), open circles represent samples taken pre-dose on cycle 1 day 15 (n=22/n=22). All patients with data as of February 2021 were included in the analysis and grouped by dosing cohort. In panel C, preliminary mean plasma concentrations following a single dose of RBN-2397 on Cycle 1 day 1 of dosing in patients show linear exposure between 100 and 500 mg RBN-2397. BID dosing commenced at Cycle 1 day 2 for all patients.

CD8$^+$ T cells, M1 macrophages, and monocytes are all increased in on-treatment biopsies of 2 patients with NSCLC treated with RBN-2397

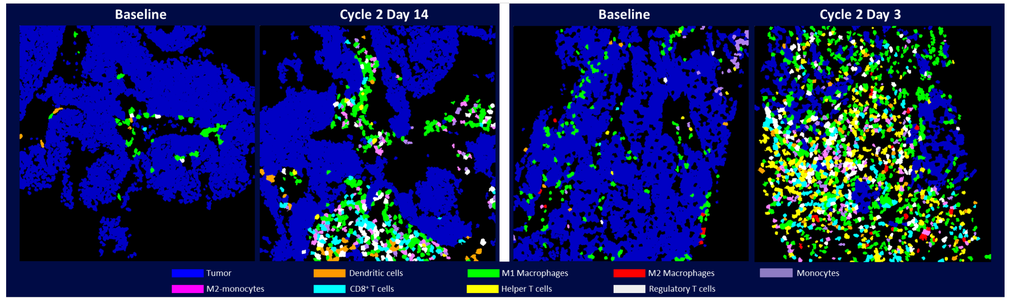

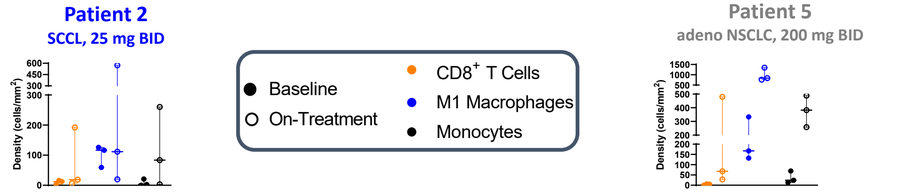

Figure 5. MIBI-TOF cell classification images illustrate infiltration of multiple T cell populations, M1 macrophages, and monocytes into the tumor regions of on-treatment biopsies from the baseline and on-treatment biopsies of two patients with NSCLC, Patient 2 (left) and Patient 5 (right). Quantification of the density of each cell type for three regions of interest per sample is shown on the right. Closed circles indicate baseline samples, open circles indicate on-treatment samples.

Induction of the adaptive immune response supports combination with immune checkpoint inhibitors in SCCL

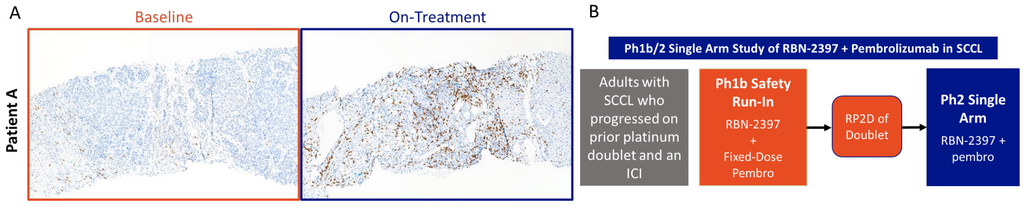

Figure 6. Panel A shows representative 10x images from immunohistochemical staining of CD8 (brown) and Granzyme B (teal) expression in the paired biopsies of an SCCL patient from the expansion cohorts of the Phase 1 study, taken at baseline and on-treatment (Cycle 1 Day 21) from a liver mass. Panel B illustrates the design of the on-going global Phase 1b/2 combination study with RBN-2397 and pembrolizumab in SCCL patients who have progressed on prior platinum doublet and an immune checkpoint inhibitor (ICI) (NCT05127590).

Conclusion

- **RBN-2397 induces tumor-specific IFN pathway activation and increases immune cell infiltration into patient tumors, providing evidence for the induction of an adaptive immune response.**
- **This confirms the tumor-intrinsic, immunomodulatory mechanism of action of RBN-2397, and supports combination studies with immune checkpoint inhibitors.**
- **A Phase 1b/2 trial of RBN-2397 in combination with pembrolizumab in SCCL patients is currently enrolling (NCT05127590).**

The authors would like to thank the patients and their families, investigators, co-investigators, and the study teams at each of the participating centers.